Mol. Cells *33*, 229-233, March 31, 2012
DOI/10.1007/s10059-012-2200-x

Molecules and Cells

High-Resolution Structure of Shikimate Dehydrogenase from *Thermotoga maritima* Reveals a Tightly Closed Conformation

Hyung Ho Lee[1,2,*]

Shikimate dehydrogenase (SDH), which catalyses the NADPH-dependent reduction of 3-dehydroshikimate to shikimate in the shikimate pathway, is an attractive target for the development of herbicides and antimicrobial agents. Structural analysis of a SDH from *Thermotoga maritima* encoded by the *Tm0346* gene was performed to facilitate further structural comparisons between the various shikimate dehydrogenases. The crystal structure of SDH from *T. maritima* was determined at 1.45 Å by molecular replacement. SDH from *T. maritima* showed a monomeric architecture. The overall structure of SDH from *T. maritima* comprises the N-terminal α/β sandwich domain for substrate binding and the C-terminal domain for NADP binding. When the *T. maritima* SDH structure was compared with those of the SDHs from other species, the SDH from *T. maritima* was in a tightly closed conformation, which should be open for catalysis. Notably, α7 moves toward the active site (~5 Å), which forces the SDH of *T. maritima* in a more closed form. Four ammonium sulfate (AMS) ions were identified in the structure. They were located in the active site and appeared to mimic the role of the substrate in terms of the enzyme activity and stability. The new high resolution structural information reported in this study, including the AMS binding sites as a potent inhibitor binding site of SDHs, is expected to supplement the existing structural data and will be useful for structure-based antibacterial discovery against SDHs.

INTRODUCTION

The shikimate pathway is an attractive target for the development of antibacterial agents because it is essential in higher plants, bacteria and fungi, but is absent in mammals (Davies et al., 1994). The shikimate pathway consists of seven enzymatic steps. The initial step is the condensation of phosphoenolpyruvate and erythrose-4-phosphate by 3-deoxy-d-arabino-heptolosonate 7-phosphate synthase (Singh et al., 2005). The fourth reaction of the shikimate pathway, which is carried out by shikimate dehydrogenase (SDH; EC 1.1.1.25) encoded by the aroE gene in bacteria, catalyses the NADPH-dependent reduction of 3-dehydroshikimate to shikimate (Singh et al., 2005). Inhibitors targeting SDH from *Helicobacter pylori* inhibit cell growth, suggesting that SDH might be a promising target for antibacterial agents (Han et al., 1997; 2006). There are two types of shikimate dehydrogenase from bacteria, SDH (PDB code 1nyt) and YdiB (PDB code 1o9b), and the crystal structures of both have been determined (Han et al., 2006).

The crystal structure of a novel shikimate dehydrogenase from *Haemophilus influenzae* revealed different kinetic properties from those of SDH and YdiB (Singh et al., 2005). The substrate specificity of SDH and YdiB is different. The SDH of *H. influenzae* catalyzes the oxidation of shikimate but not quinate, whereas YdiB catalyzes the reversible reductions of dehydroquinate to quinate and dehydroshikimate to shikimate in the presence of either NADH or NADPH (Singh et al., 2005). The oligomeric states of SDHs also differ according to the species. SDH in *Escherichia coli* is present as a monomer, whereas SDHs normally form oligomers in most bacteria (Anton and Coggins, 1988; Chaudhuri and Coggins, 1985). In comparison, SDH of *Methanococcus jannaschii* and YdiB of *E. coli* exist as dimers in both solution and crystal form (Michel et al., 2003; Padyana and Burley, 2003). The monomeric SDH is composed of two domains. The NADPH-binding domain has a typical Rossmann fold as well as a unique glycine-rich P-loop with a conserved sequence motif of GAGGXX, whereas the catalytic domain shows a novel fold (Ye et al., 2003). Subsequently, several crystal structures of SDHs have been reported including the structures of SDHs from *Staphylococcus epidermidis* (Han et al., 2009), *Thermus thermophilus* (Bagautdinov and Kunishima, 2007), *Aquifex aeolicus* (Gan et al., 2007), and *Arabidopsis* (Singh and Christendat, 2006). SDHs have two conformations, open and closed. A ternary complex of SDH from *T. thermophilus*, $NADP^+$, and shikimic acid shows an open conformation, whereas the crystal structure of SDH from *A. aeolicus* in the complex with $NADP^+$ and shikimic acid exhibits a closed conformation (Gan et al., 2007).

The three-dimensional structure of an SDH from *T. maritima* (*Tm0346*), which shares moderate levels of amino-acid sequence identity, was examined to facilitate further structural

[1]Department of Bio and Nano Chemistry, Kookmin University, Seoul 136-702, Korea, [2]Department of Integrative Biomedical Science and Engineering, Kookmin University, Seoul 136-702, Korea
*Correspondence: hhlee@kookmin.ac.kr

Received September 21, 2011; revised October 14, 2011; accepted October 17, 2011; published online November 15, 2011

Keywords: aroE, shikimate dehydrogenase, shikimate pathway, *Thermotoga maritima*

comparisons between the SDHs including any conformational changes. When the sequence of SDH from *T. maritima* was compared with those of the structurally characterized SDHs, the sequence identity was 27% against SDH from *E. coli*, 27% against YdiB from *E. coli*, 27% against SDH from *H. influenzae*, and 31% against SDH from *M. jannaschii*. The SDH from *T. maritima* (*Tm0346*) has been overexpressed in *E. coli* and crystallized. The structural details observed from the high resolution structure of *T. mariti-ma* SDH may facilitate the design of inhibitors targeting SDHs.

MATERIALS AND METHODS

Protein expression, purification, and crystallization

Protein expression, purification, crystallization, and data collection from a native crystal have been described previously (Lee, 2011). Briefly, SDH from *T. maritima* was overexpressed in *E. coli* and crystallized at 296 K using AMS as a precipitant. The crystals grew up to dimensions of 0.10 × 0.10 × 0.15 mm within six months. Crystals of SDH from *T. maritima* diffracted to a 1.45 Å resolution and belong to the orthorhombic space group $P2_12_12_1$, with unit cell parameters of a = 54.21 Å, b = 62.45 Å, and c = 68.68 Å (Lee, 2011).

Structure determination and refinement

The structure was solved by the molecular replacement method using monomer A of *E. coli* SDH (PDB ID: 1NYT) as the probe. A Cross-rotation search followed by a translation search was performed using the program CNS (Brünger et al., 1998). Subsequent manual model building was performed using the program O (Jones et al., 1991). The model was refined using the program CNS, and several rounds of model building, simulated annealing, positional refinement, and individual *B*-factor refinement were performed. The non-crystallographic symmetry restraints were relaxed in successive rounds of refinement. Water molecules were added using the program CNS, followed by a visual inspection, positional refinement, and *B*-factor refine-ment. The atomic coordinates and the structure factors were deposited in the Protein Data Bank (Accession Codes 3U62).

RESULTS AND DISCUSSION

Overall structure

The structure was solved by the molecular displacement method using the monomer model of SDH from *E. coli* (Michel et al., 2003). The structure was refined to a 1.45 Å resolution to an R_{work} and R_{free} of 19.6 and 20.1%, respectively (Table 1). The asymmetric unit contains one SDH molecule. The final model of the apo enzyme accounts for 253 residues of 253 residues, 4 AMS molecules, and 122 water molecules. The SDH from *T. maritima* has a bipartite architecture with a deep interdomain cleft: a N-terminal catalytic domain (CD) and a C-terminal NADPH binding domain (ND) (Fig. 1A). The CD consists of six β strands (β1-β6) forming a twisted β sheet with four α helices (α1-α4). The overall structure of CD is a three-layered α-β-α sandwich. The β4 strand is antiparallel to the reminder of the strands. The ND of SDH belongs to the superfamily of the NAD(P) binding Rossmann fold domains (Fig. 1A). The center of ND is a six-stranded twisted and parallel β sheet (β7-β12) with loops and α helices surrounding the core β sheet. Four AMS molecules are coordinated around the SDH from *T. maritima* in the cleft between the CD and ND *via* salt bridges and hydrogen bonding interactions. Among the four AMS molecules, AMS1 and AMS2 reside inside ND, whereas AMS3 and AMS4 make contact with both CD and ND. This may function to improve the diffraction quality of the crystals.

Table 1. Model refinement statistics

Resolution range (Å)	20-1.45
R_{work} / R_{free}[a] (%)	19.6 / 20.1
No. of nonhydrogen atoms / average *B*-factor (Å^2)	
Protein	2 035 / 14.4
Ammonium sulfate	4 × AMS / 18.5
Water	122 / 23.6
r.m.s. deviations from ideal geometry	
Bond lengths (Å) / bond angles (°)	0.0063 / 0.99
Ramachandran plot	
Most favorable (%)	96.4
Allowed (%)	3.6
Generously allowed (%)	0
PDB code	3U62

[a] $R = \Sigma \mid |F_{obs}| - |F_{calc}| \mid / \Sigma |F_{obs}|$, where R_{free} was calculated for a randomly chosen 10% of reflections, which were not used for structure refinement and R_{work} was calculated for the remaining reflections.

Oligomeric state and structural comparison

Gel-filtration and crystallographic data confirmed that *T. maritima* SDH exists as a monomer in both crystal and solution states (data not shown). When *T. maritima* SDH structure was compared with monomer A of *E. coli* SDH (PDB ID: 1NYT), monomer A of *H. influenzae* SDH (PDB ID: 1P74), monomer A of *M. jannaschii* SDH (PDB ID: 1NVT), monomer A of *S. epidermidis* SDH (PDB ID: 3DON), monomer A of *T. thermophilus* SDH (PDB ID: 2D5C), monomer A of *A. aeolicus* SDH (PDB ID: 2HK8), and monomer A of *Arabidopsis* SDH (PDB ID: 2GPT), the root mean square (r.m.s.) deviations range 2.2 Å for 211 Cα atom pairs, 3.1 Å for 198 Cα atom pairs, 2.8 Å for 209 Cα atom pairs, 3.4 Å for 225 Cα atom pairs, 1.5 Å for 204 Cα atom pairs, 1.5 Å for 194 Cα atom pairs, and 1.9 Å for 184 Cα atom pairs, respectively, which showed good structural similarity (Fig. 1B).

SDH has two types of conformations, namely the open and closed forms. The closed form is believed to be necessary for catalysis (Michel et al., 2003). In the case of SDH from *E. coli*, there is a switch from the open to the closed conformation upon substrate binding (Michel et al., 2003). In SDH from *T. thermophilus*, the cofactor only binds to the closed form, whereas the substrate binds to both forms (Bagautdinov and Kunishima, 2007). The structure of SDH from *S. epidermidis* shows the most open form of all known SDHs (Han et al., 2009). To confirm the conformation of SDH from *T. maritima*, the SDH from *T. maritima* was superimposed with SDHs in the open and closed forms (Fig. 1B). In particular, α7 moves toward the active site (~5 Å), which forces the SDH of *T. maritima* in a more closed form (Fig. 1B). The conformational difference is also observed in the C-terminal α12, which is more closed than that of *T. thermophilus* SDH.

AMS coordination

The four AMS molecules are clearly defined by electron density and is bound near the active site (Fig. 1). The mean B-factors of the four AMS molecules (AMS1, AMS2, AMS3, and AMS4) are 21.5, 16.0, 11.6, and 24.8 Å^2, respectively. The side chains of Arg140, Arg144, and Ser175 as well as the backbone

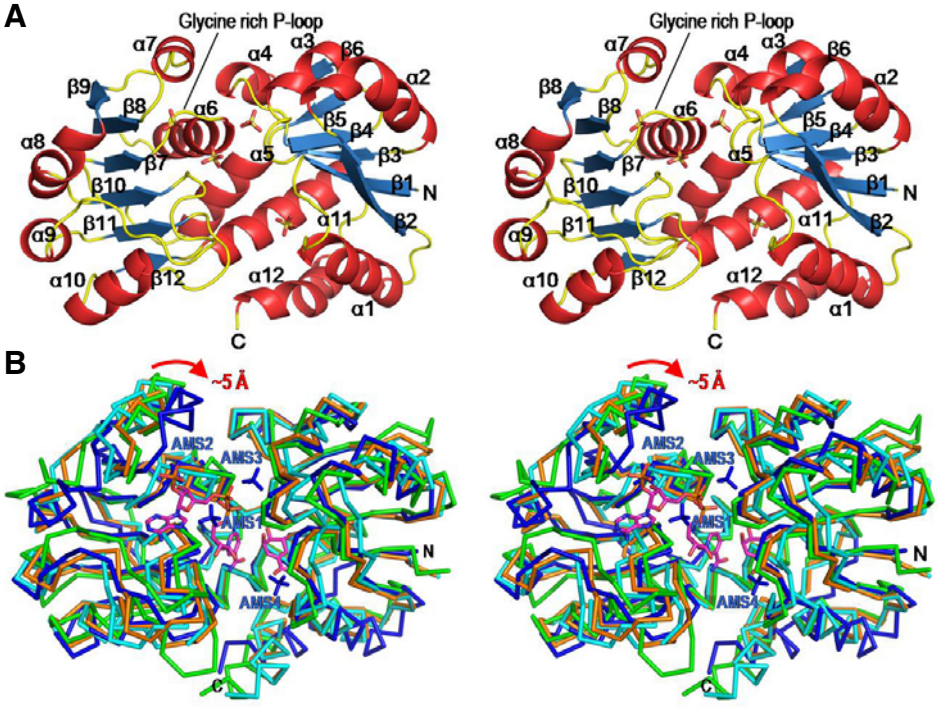

Fig. 1. Overall structure of *T. maritima* SDH. (A) Stereo view of ribbon diagram of *T. maritima* SDH. Each secondary element is in different colors. The secondary structure elements were defined by PyMOL (The PyMOL Molecular Graphics System, http://www.pymol.org). (B) Stereo view of superposition of *T. maritima* SDH (blue) and other SDHs. The four AMS molecules and Cα trace of *T. maritima* SDH are colored in blue. *E. coli* SDH (PDB ID: 1NYT, monomer A in a closed form) (Michel et al., 2003) is colored in green, and SDHs from *T. thermophilus* are colored in orange (PDB ID: 2D5C, monomer A in a closed form) and cyan (PDB ID: 2CY0, monomer B in an open form), respectively (Bagautdinov and Kunishima, 2007). Both NADP(H) (PDB ID: 1NYT, monomer A) and shikimate (PDB ID: 2D5C, monomer A) are shown as magenta sticks.

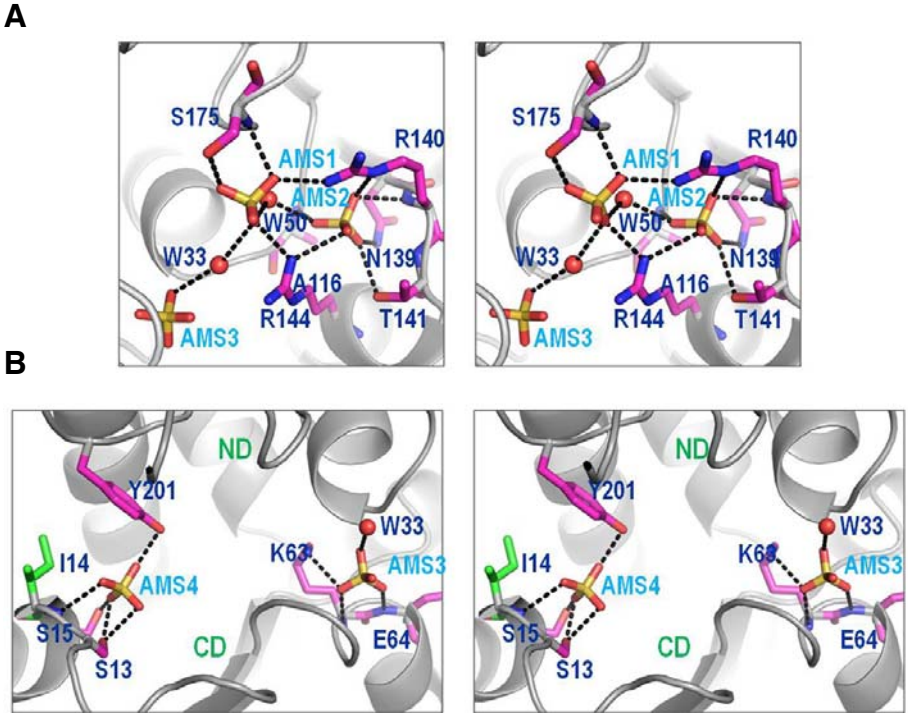

Fig. 2. A close-up stereo view of a AMS binding to *T. maritima* SDH. (A) Residues near the AMS molecules (AMS1, AMS2, and AMS3) are shown as sticks. The black dotted lines de-note hydrogen bonds. The red balls represent the water molecules. (B) The residues near the AMS molecules (AMS3 and AMS4) are shown in sticks. The black dotted lines denote the hydrogen bonds. The red balls represent water molecules.

nitrogen of Ser175 interact directly with AMS1 (Fig. 2A). Two water molecules (W33 and W50) are also bound to AMS1. The O3 atom of AMS1 makes two direct contacts with both the backbone nitrogen atom of Ser175 (2.9 Å) and the NH2 atom of Arg140 (2.9 Å), whereas the O4 atom of AMS1 is hydrogen-bonded to the OG atom of Ser175 (2.6 Å). The separation between the O2 atom of AMS1 and the Arg144 NH1 atom is 2.9 Å. Two water molecules (W33 and W50) are also hydrogen-bonded to the O2 atom of AMS1 (3.2 Å and 2.8 Å, respectively) (Fig. 2A). The side chains of Asn139, Arg140, Thr141, and Arg144 as well as the backbone nitrogen atoms of Ala116 and Arg140 interact directly with AMS2 (Fig. 2A). One water

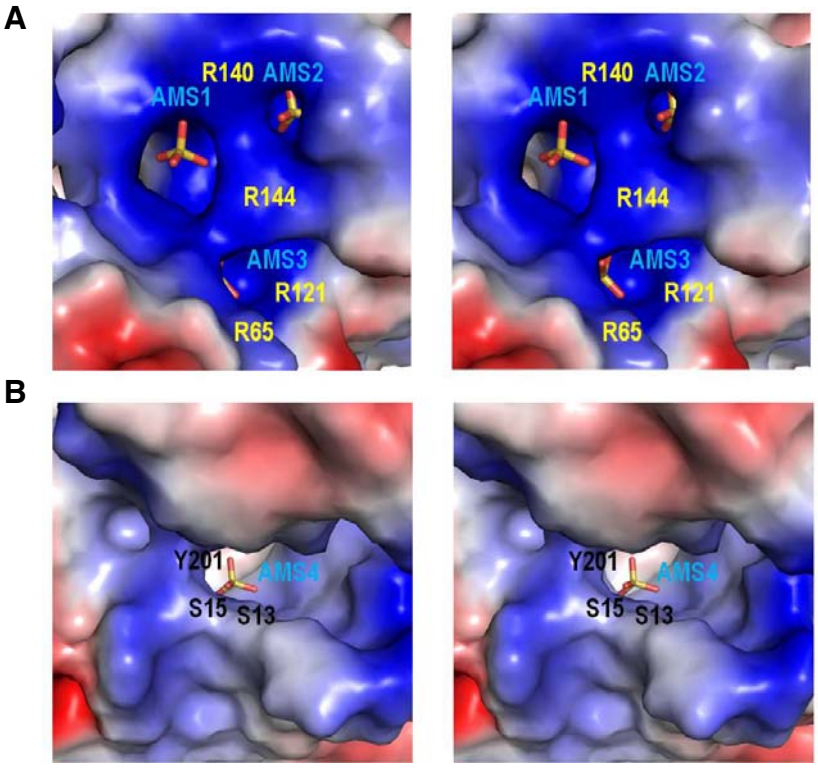

Fig. 3. A surface view of AMS binding. (A) Stereo view of the electrostatic potential at the molecular surface of *T. maritima* SDH around the AMS1, AMS2, and AMS3 binding pockets. (B) Stereo view of the electrostatic potential at the molecular surface of *T. maritima* SDH around the AMS4 binding pocket.

molecule (W50) is also bound to AMS2. The O1 atom of AMS2 makes direct contact with the NH1 atom of Arg144 (3.1 Å), whereas the O2 atom of AMS2 is bound to both the OG1 atom of Thr141 (3.0 Å) and the ND2 atom of Asn139 (2.9 Å). The O3 atom of AMS2 makes two hydrogen bonds with both the NE atom (3.0 Å) and the backbone nitrogen atom of Arg140 (2.9 Å), whereas the O4 atom of AMS2 is hydrogen-bonded through a water molecule (W50, 3.0 Å) and the backbone nitrogen atom of Ala116 (2.8 Å) (Fig. 2A).

AMS3 is bound near the AMS1 binding site (Fig. 2A) and interacts with AMS1 indirectly through a water molecule (W33), which means that AMS3 interacts with ND indirectly. The distance between the O3 atom of AMS3 and W33 is 3.0 Å. The side chain of Lys63 as well as the backbone nitrogen atoms of Lys63 and Glu64 interacts directly with AMS3 (Fig. 2B). The two backbone nitrogen atoms of Lys63 and Glu64 are hydrogen-bonded to the O4 atom (2.9 Å) and O2 atom (3.0 Å), respectively, whereas the O4 atom of AMS3 makes a salt bridge with the NZ atom of Lys63 (2.8 Å). The side chains of Ser13 and Tyr201 as well as the backbone nitrogen of Ile14 interact directly with AMS4 (Fig. 2B). The O1 atom of AMS4 makes direct hydrogen bonds with the backbone nitrogen atom of Ile14 (3.0 Å), whereas the O2 atom of AMS4 is hydrogen-bonded to the OG atom of Ser13 (2.9 Å). The separation between the O3 atom of AMS4 and the Tyr201 OH group is 2.5 Å. The O4 atom of AMS4 makes two direct contacts with both the OG atoms of Ser13 (2.9 Å) and Ser15 (2.6 Å). AMS1, AMS2, and AMS3 reside on the surface patch with a highly positive electrostatic potential due to the clustering of positively charged residues (Arg65, Arg121, Arg140, and Arg144) (Fig. 3).

Structural insight into substrate binding

The shikimate and NADP(H) molecules of SDH from *T. thermophilus* were incorporated into the *T. maritima* SDH structure to determine if the AMS binding sites are near the substrate or cofactor binding sites (Fig. 1B). Indeed, many of the substrate or cofactor binding residues interact with the AMS molecules. Ala124 (Ala116 in *T. maritima* SDH), Asn146 (Asn139 in *T. maritima* SDH), Arg147 (Arg140 in *T. maritima* SDH), Arg151 (Arg144 in *T. maritima* SDH), and Arg180 (Ser175 in *T. maritima* SDH) are involved in the recognition of NADH in SDH of *T. thermophilus* (Bagautdinov and Kunishima, 2007). Among the residues interacting with NADH, Ala116 and Arg144 in *T. maritima* SDH are coordinated with AMS2, whereas Arg140, Arg144, and Ser175 interact with AMS1 (Fig. 2A). The position of AMS1 appears to mimic the position of the PA-phosphate group of NADP(H) (Fig. 1B). Arg140 of *T. maritima* SDH interacts directly with AMS1, whereas Arg147 of *T. thermophilus* SDH (the corresponding residue of Arg140 in *T. maritima* SDH) is involved in the recognition of the PA-phosphate group of NADH (Bagautdinov and Kunishima, 2007). The position of AMS2 appears to mimic the position of the P2B-phosphate group of NADP(H) (Fig. 1B). Ala116 of *T. maritima* SDH makes contact with AMS2, whereas Ala124 *T. thermophilus* SDH (the corresponding residue of Ala116 in *T. maritima* SDH) is involved in the recognition of the P2B -phosphate group of NADH (Bagautdinov and Kunishima, 2007). The position of AMS4 appears to mimic the shikimate binding site (Fig. 1B). Both Ser13 and Ser15 of *T. maritima* SDH, which are crucial residues for AMS4 binding, are also conserved substrate binding residues in *T. thermophilus* SDH (Bagautdinov and Kunishima, 2007).

In conclusion, structural analysis of the SDH from *T. maritima* was performed. The results indicate that the preferred oligomeric state of the SDH from *T. maritima* is a monomer. Based on the structure, four AMS molecules are positioned in the cleft between the ND and CD via salt bridges and hydrogen bonding interactions and stabilize the monomer conformation. The data

also showed that SDH from *T. maritima* has a tightly closed conformation. It is believed that the high resolution structure of SDH from *T. maritima* together with AMS coordination will provide useful information that will enable an inhibitor design that targets the active site.

ACKNOWLEDGMENTS

The author wishes to thank Dr. Se Won Suh for supporting this work in all aspects and the staff at beamline BL-6B of Pohang Light Source for their assistance during the X-ray experiments. This study was supported by the National Research Foundation of Korea grant funded by the Korean government Ministry of Education, Science and Technology (grant no. 2011-0005805) and by the Research Program 2011 of Kookmin University to HHL. This work was also supported by the Seoul R&BD program (ST100072) to HHL.

REFERENCES

Anton, I.A., and Coggins, J.R. (1988). Sequencing and overexpression of the *Escherichia coli* aroE gene encoding shikimate dehydrogenase. Biochem. J. *249*, 319-326.

Bagautdinov, B., and Kunishima, N. (2007). Crystal structures of shikimate dehydrogenase AroE from *Thermus thermophilus* HB8 and its cofactor and substrate complexes: insights into the enzymatic mechanism. J. Mol. Biol. *373*, 424-438.

Brünger, A.T., Adams, P.D., Clore, G.M., DeLano, W.L., Gros, P., Grosse-Kunstleve, R.W., Jiang, J.S., Kuszewski, J., Nilges, M., Pannu, N.S., et al. (1998). Crystallography & NMR system: A new software suite for macromolecular structure determination. Acta Crystallogr. Sect. D Biol. Crystallogr. *54*, 905-921.

Chaudhuri, S., and Coggins, J.R. (1985). The purification of shikimate dehydrogenase from *Escherichia coli*. Biochem. J. *226*, 217-223.

Davies, G.M., Barrett-Bee, K.J., Jude, D.A., Lehan, M., Nichols, W.W., Pinder, P.E., Thain, J.L., Watkins, W.J., and Wilson, R.G. (1994). (6S)-6-fluoroshikimic acid, an antibacterial agent acting on the aromatic biosynthetic pathway. Antimicrob. Agents Chemother. *38*, 403-406.

Gan, J., Wu, Y., Prabakaran, P., Gu, Y., Li, Y., Andrykovitch, M., Liu, H., Gong, Y., Yan, H., and Ji, X. (2007). Structural and bio-chemical analyses of shikimate dehydrogenase AroE from *Aquifex aeolicus*: implications for the catalytic mechanism. Biochemistry *46*, 9513-9522.

Han, J., Yu, E., Lee, I., and Lee, Y. (1997). Diversity among clinical isolates of Helicobacter pylori in Korea. Mol. Cells *7*, 544-547.

Han, C., Wang, L., Yu, K., Chen, L., Hu, L., Chen, K., Jiang, H., and Shen, X. (2006). Biochemical characterization and inhibitor discovery of shikimate dehydrogenase from *Helicobacter pylori*. FEBS J. *273*, 4682-4692.

Han, C., Hu, T., Wu, D., Qu, S., Zhou, J., Ding, J., Shen, X., Qu, D., and Jiang, H. (2009). X-ray crystallographic and enzymatic analyses of shikimate dehydrogenase from *Staphylococcus epidermidis*. FEBS J. *276*, 1125-1139.

Jones, T.A., Zou, J.Y., Cowan, S.W., and Kjeldgaard, M. (1991). Improved methods for building protein models in electron density maps and the location of errors in these models. Acta Crystallogr. Sect. A *47*, 110-119.

Lee, H.H. (2011). Overexpression, crystallization, and preliminary X-ray crystallographic analysis of shikimate dehydrogenase from *Thermotoga maritima*. Acta. Crystallogr. Sect. F. Struct. Biol. Cryst. Commun. *67*, 824-826.

Michel, G., Roszak, A.W., Sauve, V., Maclean, J., Matte, A., Coggins, J.R., Cygler, M., and Lapthorn, A.J. (2003). Structures of shikimate dehydrogenase AroE and its Paralog YdiB. A common structural framework for different activities. J. Biol. Chem. *278*, 19463-19472.

Padyana, A.K., and Burley, S.K. (2003). Crystal structure of shikimate 5-dehydrogenase (SDH) bound to NADP: insights into function and evolution. Structure *11*, 1005-1013.

Singh, S.A., and Christendat, D. (2006). Structure of Arabidopsis dehydroquinate dehydratase-shikimate dehydrogenase and implications for metabolic channeling in the shikimate pathway. Biochemistry *45*, 7787-7796.

Singh, S., Korolev, S., Koroleva, O., Zarembinski, T., Collart, F., Joachimiak, A., and Christendat, D. (2005). Crystal structure of a novel shikimate dehydrogenase from *Haemophilus influenzae*. J. Biol. Chem. *280*, 17101-17108.

Ye, S., Von Delft, F., Brooun, A., Knuth, M.W., Swanson, R.V., and McRee, D.E. (2003). The crystal structure of shikimate dehydrogenase (AroE) reveals a unique NADPH binding mode. J. Bacteriol. *185*, 4144-4151.